

CHAPTER V
SCALING OF YIELD STRESS OF POLYTHIOPHENE SUSPENSIONS
UNDER ELECTRIC FIELD

5.1 Abstract

Electrorheological properties in steady shear of perchloric acid doped poly(3-thiophene acetic acid), PTAA, particles in silicone oil were investigated to determine the effects of field strength, particle concentration, doping degree (conductivity values), operating temperature, and nonionic surfactant. The PTAA/silicone oil suspensions show the typical ER response of Bingham flow behavior upon the application of electric field. The yield stress increases with electric field strength, E , and particle volume fraction, ϕ , according to a scaling law of the form, $\tau_y \propto E^\alpha \phi^\gamma$. The scaling exponent α approaches the value of 2, predicted by the polarization model, as the particle volume fraction decreases and when the doping level of the particles decreases. The scaling exponent γ tends to unity, as predicted by the polarization model, when the electric field strength is low. The yield stress under electric field initially increases with temperature up to 25 °C, and then levels off. At electric fields above of 1.5 kV/mm, the yield stress increases significantly by up to 50% on addition of small amounts of a nonionic surfactant.

KEYWORDS: Conducting polymers, Electrorheological fluid, Polythiophene, Steady-State shear, Yield stress

5.2 Introduction

Electrorheological (ER) fluids are suspensions that exhibit a dramatic change in rheological properties due to the application of electric field. Commonly, they are composed of polarizable particles dispersed in a non-conducting fluid. Upon the application of an electric field, chain-like or fibrillar aggregates of the suspended particles are oriented along the direction of the electric field, thereby inducing viscoelasticity and a drastic increase in viscosity (Sakurai *et al.*, 1999). ER fluid response is much faster than that of conventional mechanical systems and offers great potential for various hydraulic engineering applications, as the active elements of clutches, breaks, shock absorbers, engine mounts, and dampers (Voyles *et al.*, 1996, Kamath and Wereley, 1997, Mavroidis *et al.*, 2000).

Typically, the steady-state rheological properties have been investigated for most ER fluids (Klingenberg and Zukoski, 1990, Bonnecaze and Brady, 1992, Choi *et al.*, 1998, Chin *et al.*, 1999, Choi, 1999, Gozdzalik *et al.*, 2000, Sohn *et al.*, 2002, Langavola *et al.*, 2003, Zhao and Yin, 2002). The steady-state rheological response in shearing flows is commonly modeled as a Bingham fluid (Sung *et al.*, 2003, Rankin and Klingenberg, 1998), with an electric field dependent yield stress, $\tau_y(E_o)$,

$$\begin{aligned} \tau(\dot{\gamma}, E_o) &= \tau_y(E_o) + \eta\dot{\gamma} & \tau \geq \tau_y, \\ \dot{\gamma} &= 0 & \tau < \tau_y, \end{aligned} \quad (5.1)$$

where τ is the shear stress, τ_y is the yield stress, E_o is the applied field strength, η is the shear viscosity, and $\dot{\gamma}$ is the shear rate.

Recently, there has been interest in using conductive polymers as suspended particles for dry-base ER fluids. Conductive polymers can offer a variety of advantages for ER systems: better thermal stability, insolubility, and more controllable viscosity. Suspensions of conductive polymers exhibit intrinsic ER properties without the necessity to introduce other additives. The polarization is induced by the motion of electrons within the suspended particles under application of electric field. Various conductive polymers have been tested as particulate

materials in ER systems. Examples include polyaniline (PANI) and its derivatives (Jang *et al.*, 2001, Kim *et al.*, 2000, Lee *et al.*, 1999, Krause and Bohon, 1998, Lee *et al.*, 1998), PANI copolymers (Lee *et al.*, 2001, Cho *et al.*, 2000, Jun *et al.*, 2002, Choi *et al.*, 2001), polypyrrole (Kim and Park, 2002, Goodwin *et al.*, 1997), poly (acene quinone) radical (Choi *et al.*, 2001), poly (naphthalene quinone) radical (Cho and Choi, 2000), and poly (p-phenylene) (Choi *et al.*, 2001, Sim *et al.*, 2001).

In this study, we explore the ER behavior of Poly (3-thiophene acetic acid) (PTAA), doped with perchloric acid (HClO₄) to vary the conductivity. The static yield stress of HClO₄-doped PTAA suspensions were investigated in the presence and absence of applied electric fields. The effect of field strength, particle concentration, doping degree (conductivity values), operating temperature, and nonionic surfactant on the yield stress was investigated.

5.3 Experimental

5.3.1 Materials

3-thiopheneacetic acid, 3TAA (AR grade, Fluka) was used as the monomer. Anhydrous ferric chloride, FeCl₃ (AR grade, Riedel-de Haen) was used as the oxidant. Chloroform, CHCl₃ (AR grade, Lab-Scan) and methanol, CH₃OH (AR grade, Lab-Scan) were dried over CaH₂ for 24 hours under the nitrogen atmosphere and then distilled. The perchloric acid dopant, HClO₄ (AR grade, AnalaR) was used as received. The dispersing phase was silicone oil (AR grade, Dow corning) with density 0.96 g/cm³ and kinematic viscosity of 100 cSt, and was vacuum-dried and stored in a desiccator prior to use. Polyoxyethylene sorbitanmonolaurate, Tween 20 (AR grade, Fluka) was used as received.

5.3.2 Synthesis of Poly (3-thiopheneacetic acid)

Poly (3-thiopheneacetic acid), PTAA was synthesized by oxidative-coupling polymerization according to the method of Kim *et al.* (Kim *et al.*, 1999). 10.0 g of 3-thiopheneacetic acid was refluxed for 24 hours in 50 ml of dry methanol with 1 drop of concentrated H₂SO₄, to protect against the oxidative decomposition of the carboxylic acid group of monomer during polymerization. The methanol was

evaporated, and the residue was extracted with diethyl ether. The extract was washed with deionized water, dried with anhydrous MgSO_4 , and then filtered. The diethyl ether was evaporated from the filtrate by rotating evaporator.

A solution of 10 mmol of protected monomer in 20 ml of chloroform was added dropwise to a solution of 40 mmol of ferric chloride in 30 ml of chloroform under nitrogen atmosphere. The reaction was carefully maintained at 0°C ($\pm 0.5^\circ\text{C}$) for 24 hours. The reaction mixture was precipitated, by pouring into a large excess amount of methanol. The precipitate was repeatedly washed with methanol and deionized water. The precipitate was hydrolyzed, by heating 0.5 g precipitate in 50 ml of 2.0 M NaOH solution for 24 hours at 100°C . The PTAA obtained was neutralized and precipitated with a dilute HCl solution. The PTAA was washed several times with deionized water before vacuum drying at room temperature for 2 days.

To examine the effect of particle conductivity on the electrorheological properties, PTAA particles having different conductivity values were prepared by doping with perchloric acid (Chen *et al.*, 2000). HClO_4 doped PTAA was prepared by stirring ground PTAA (~ 7.04 mmol) with HClO_4 aqueous solution at room temperature for 3 days. The amounts of acid used were 7.04 ml of ~ 0.1 M aqueous acid and 176 ml of ~ 4.0 M aqueous acid for low and high doping ratios (mole of acid:mole of monomer unit) of 1.09×10^{-3} and 0.255, respectively. These values represent theoretical upper bounds based on the mixing conditions. The HClO_4 doped PTAA particles were filtered and vacuum-dried for 24 hours before grinding with a mortar and a pestle and then passed through a $38\ \mu\text{m}$ sieve shaker to control the particle size distribution.

5.3.3 Conductivity Measurement

For the conductivity measurement, HClO_4 doped polythiophene disks (25 mm diameter and ~ 0.2 mm thickness) were prepared by molding in a hydraulic press. Electrical conductivity was measured using a custom-built four-point probe. The specific conductivity, σ (S/cm), was obtained, by measuring the resistance, R , and using the following relation: $\sigma = (1/Rt)(l/K)$, where t is the disk thickness and K

is a geometric correction factor. The geometric correlation factor was calibrated using standard silicon wafer sheets of known specific resistivities. The measurements were performed in the linear Ohmic regime i.e. the specific conductivity values were independent of the applied DC current. The measurements were carried out at 25 °C and repeated at least two times.

5.3.4 Preparation of ER Fluid and ER Measurements

The electrorheological, ER, fluids were prepared by dispersing HClO₄ doped PTAA particles in silicone oil (density 0.96 g/cm³ and kinematic viscosity 100 cSt) with ultrasonicator for 30 minutes at 25 °C.

Rheological properties were carried out using a rotational rheometer (Carrimed, CR50) with 4 cm diameter parallel plate geometry at 25 ± 0.1 °C. The gap for the geometry used was 0.1 mm for each measurement. A DC voltage was applied during the rheological measurements using a high voltage power supply (Bertan Associates Inc., Model 215). The electric field was applied for 10 minutes to ensure the formation of equilibrium agglomerate structure before a measurement was taken. Each measurement was carried out at a temperature of 25 ± 0.1 °C and repeated at least two or three times. The static yield stress was measured using the controlled shear stress mode (CSS) as the highest stress value prior to the onset of flow in the presence of an electric field of specified magnitude. CSS experiments were also applied to investigate the dependence of viscosity on shear stress above the yield point. In the CSS experiments, the shear sweep was always applied at a sweep rate of 40 Pa/min.

5.3.5 Microscope Observation

The morphology of the PTAA particles was characterized using scanning electron microscopy (JEOL, JSM-5200-2AE), using an acceleration voltage of 20 kV and a magnification of 1,000. The formation of particle chain structures in the electric field under stationary conditions was observed with an optical microscope (B&B Microscopes, Ltd., Olympus BX60) equipped with a camera (Diagonostic Instrument Inc., model # 3.2.0). ER fluids were placed between

stationary thin copper foil electrodes attached to glass slides. External electric fields were applied to the suspensions using a DC power supply (Bertan Associates Inc., Model 215).

5.4 Results and Discussion

Previously, we have reported measurements of the mean PTAA particle diameter, determined by particle size analyzer (Malvern, Master Sizer Xv2.15) to be approximately 30 μm with a standard deviation of $\sim 8 \mu\text{m}$. SEM analysis indicates the shapes of the undoped and doped PTAA particles are quite irregular.

The effect of particle concentration and particle conductivity on the electrorheological properties of the suspensions was investigated. Particle concentrations investigated were 5%, 10%, and 20% by weight (corresponding to volume fraction of 0.025, 0.048, and 0.092, respectively) at a specific conductivity of $7.5 \times 10^{-2} \text{ S/cm}$ (HPT5, HPT10, and HPT20). To study the effect of conductivity, the particle concentration was fixed at 20% by weight and the particle conductivity values were set at zero (undoped, UPT20), $2.0 \times 10^{-4} \text{ S/cm}$ (low doping, LPT20), and $7.5 \times 10^{-2} \text{ S/cm}$ (high-doping, HPT20) S/cm, respectively.

Figure 5.1 shows the measurement of static yield stress of 5 wt % highly HClO_4 doped polythiophene suspensions at various electric field strengths. An increasing shear stress was applied until the particle chain structure is broken down, giving rise to shear flow. The stress at this point is known as the static yield stress, τ_y (Choi *et al.*, 1999).

The effect of particle concentration on static yield stress of highly HClO_4 doped polythiophene (HPT) suspensions at various electric field strengths is shown in Figure 5.2. The yield stress at specified electric field strength increases with particle concentration, and at specified concentration, increases as the electric field strength increases. For the highest concentration, 20 wt %, the static yield stress increases to approximately 370 Pa, when an electric field strength of 3 kV/mm is applied, and exceeds the measurement limit of the instrument when the field strength is higher than 3 kV/mm.

Generally, the flow behavior of ER fluids is described using the electrostatic polarization model (Klingenberg *et al.*, 1991, Klingenberg *et al.*, 1991), which arises due to the mismatch between the complex components of the dielectric permittivity of the particles and the medium. Each sphere is treated as a point dipole, located at the sphere center and aligned with the applied electric field, the magnitude of the dipole being that induced on an isolated dielectric sphere in a uniform electric field. The net force on each sphere is the sum of its interactions with all other spheres. The stress, τ , is predicted to be proportional to the square of the electric field, E^2 :

$$\tau \propto \phi K_f E^2 \beta^2 \quad (5.2)$$

where ϕ is the volume fraction of particles, K_f is the dielectric permittivity of the continuous medium, and β is the relative polarizability, which under DC or low frequency AC fields, is controlled by the conductivities of the particles and continuous medium, whereas the polarization is determined solely by the particles and medium permittivities under high frequency AC fields (Pathasarathy and Klingenberg, 1996).

From Figure 5.2, it is evident that τ_y is field independent when the field strength, E , is below 100 V/mm, and τ_y exhibits a power-law dependence on E , $\tau_y \sim E^\alpha$, when $E > 100$ V/m. The values of α deduced from the fits in Figure 5.2 are 1.94, 1.81, and 1.69, for the 5%, 10%, and 20% by weight HPT suspensions, respectively. These values evidently approach the value of 2.0, predicted by the polarization model as the volume fraction decreases. Deviation from the predicted value may arise because of the nonspherical particle shape, the effect of the particle size distribution, and/or a non-linear polarizability. Moreover, in the polarization model, the electrostatic interaction between spheres is treated in the point dipole approximation, which may be inadequate for real dispersions.

Figure 5.3 shows the effect of particle conductivity on the static yield stress of 20 wt % HClO₄ doped polythiophene suspensions at various electric field strengths. At any specified electric field strength, the yield stress increases with particle conductivity, i.e the yield stress increases in the order UPT20 < LPT20 <

HPT20. In all three systems, when $E > 100$ V/m, τ_y exhibits a power-law dependence on E , $\tau_y \sim E^\alpha$. The values of α are determined to be 1.90, 1.90, and 1.69, for UPT20, LPT20, and HPT20, respectively. The scaling exponent α evidently deviates from the predicted value of 2 as particle conductivity increases.

The influence on the static yield stress of the volume fraction of HClO₄ doped polythiophene particles in silicone oil is shown in Figure 5.4. The scaling exponent γ of the relation $\tau_y \sim \phi^\gamma$ varies from 0.95, 1.02, 0.85 and 0.73 as the electric field strength increases from 0.5, to 1.0, 2.0 and 3.0 kV/mm, respectively. Evidently, the linear relationship between the yield stress and the volume fraction holds at low electric field strength but deviation from linearity occurs at high electric field strength. This may reflect the fact that, at high volume fraction, three-dimensional structures exist in addition to linear strings of particles, as shown later.

The effect of operating temperature on the static yield stress of 20 wt % highly HClO₄ doped polythiophene suspension (HPT20) at various electric field strengths is shown in Figure 5.5. The ER properties were measured within the temperature range of 15-60 °C. The yield stress initially increases with the operating temperature. This is presumably due to enhancement of conductivity with increase of temperature (Lee *et al.*, 1998). However, the temperature dependence disappears above 30 °C. Similar anomalous temperature dependence of the yield stress has been reported previously (Jordan and Shaw, 1989, Weiss and Duclos, 1994, Wu and Conrad, 1998, Ma *et al.*, 1998, Conrad and Chen, 1995, Lan *et al.*, 1998). Diverse phenomena have been implicated in the origin of such effects (Gonon and Foulc, 2000), including the effect of Brownian motion on the structure of the suspension (Jordan and Shaw, 1989), the temperature dependence of the viscosity (Weiss and Duclos, 1994), density (Weiss and Duclos, 1994), or conductivity of the host liquid (Wu and Conrad, 1998), the temperature dependence of the solid phase permittivity (Jordan and Shaw, 1989, Ma *et al.*, 1998), or of the liquid and solid conductivities (Conrad and Chen, 1995, Lan *et al.*, 1998), or the temperature dependence of particle-particle interactions (Gonon and Foulc, 2000). Future studies will be directed to elucidate which of these effects are relevant to our system.

Frequently, surfactants are added to ER suspensions to promote colloid stability against aggregation. However, a small amount of surfactant can also enhance the ER effect (Lee *et al.*, 1998). Thus, Kim *et al.* (Kim and Klingenberg, 1996) have suggested that small concentrations of surfactants increase the yield stress by increasing the particle polarizability via enhanced interfacial polarization. In the present study, the influence of a nonionic surfactant, Tween20, on the yield stress of a 20 wt % highly HClO₄ doped polythiophene suspension (HPT20) was investigated. In Figure 5.6, the static yield stress of HPT20 is plotted versus the concentration of Tween20 at various electric field strengths. When the electric field strength is relatively weak, the yield stress does not depend on the presence of the surfactant. However, at electric fields of 1.5 kV/mm and 2 kV/mm, the yield stress increases by up to 50% as surfactant is added and then levels off at higher surfactant concentration.

Figure 5.7 exhibits the changes in viscosity of HPT20 suspension, during a stress sweep test: Figure 5.7(a) shows the steady shear viscosity plotted vs. shear stress; Figure 5.7(b) shows the complex oscillatory shear viscosity $\eta^* = \omega^{-1} \sqrt{(G')^2 + (G'')^2}$ ($\omega = 1\text{Hz}$), plotted vs. shear stress. In each case, an applied electric field of 2 kV/mm is alternately turned on and off, and the stress sweep rate utilized was 40 Pa/min. On applying and subsequently releasing the electric field, respectively, the steady state viscosity and the complex viscosity each instantaneously increase and then return to their baseline values. The magnitude of the complex viscosity is greater than that of the steady shear viscosity by almost five orders of magnitude, e.g. at a stress of 225 Pa, the increase in the steady state shear viscosity is approximately 0.24 Pa·s whereas the increase in the complex viscosity is approximately 1.6×10^4 Pa·s. As expected, the steady state shear viscosity is dramatically smaller than the complex oscillatory viscosity, because particle strings or columns are broken off in steady state shear, whereas they remain essentially intact under oscillatory shear at small strains, even when the applied stress is identical. Thus, the rheology dramatically deviates from the Cox-Mertz rule (Cox and Mertz, 1958, Barnes *et al.*, 1989), which stipulates that the complex and steady shear viscosities should have the same value at equivalent as strain rates ($\dot{\gamma}$) and

frequencies (ω). Such deviations are expected when fibrillar structures which present under small-strain oscillatory shear are disrupted under large shear strain. Also evident in Figure 5.7(a) and 5.7(b), the magnitude of the increase in steady shear viscosity and complex oscillatory viscosity of HPT20 suspensions on application of the electric field decreases with increasing stress; i.e. the fluid exhibits strongly shear-thinning rheology in the presence of the applied field. In contrast, the rheology in the absence of the electric field is Newtonian, and the Cox-Mertz rule is obeyed, i.e. $\eta(\dot{\gamma}) = \eta(\omega) = 0.12 \text{ Pa}\cdot\text{s}$. In summary, the ER enhancement of viscosity is much greater at low shear strains. Application of large strains distorts the aligned fibrillar structures, leads to a fragmentation of the chains, and results in dramatic decrease of the viscosity. Analogous, shear thinning viscometric behavior has been previously reported for other ER fluids, such as polyaniline (Bonnecaze and Brady, 1992), polyaniline-co-ethoxyaniline (Choi *et al.*, 2001), and chitosan polysaccharide (Sung *et al.*, 2003).

Optical micrographs of the 5 wt% highly doped PTAA suspension (HPT5) at increasing electric field strengths under quiescent conditions are shown in Figure 5.8. It can be seen clearly that the particles are randomly distributed at zero field, whereas on application of the electric field, a transition to an organized fibrillar structure occurs due to the long-range interacting electrostatic polarization forces. For HPT5, the fibrils are initially observed at 1 kV/mm. The density and thickness of the fibrils increases with the field strength and some branching occurs. These effects are manifested through the increased agglomeration of particles, because higher field strength increases polarization, and enhances the attractive interactions of particles (Radcliffe *et al.*, 1996). Figure 5.9 shows micrographs of HPT5, at fixed field strength of 3 kV/mm, as a function of time. When the electric field is applied, the particles are immediately polarized and within two seconds form many chains bridging the two electrodes. Relatively minor changes are observed subsequently, involving some further coalescence of particles. Figure 5.10 shows the optical micrographs of HPT suspensions with different particle concentrations as a function of electric field strength. It is evident of course that at fixed field strength, increase of concentration results in increased density of fibrillar aggregates. Also, at low

concentration (HPT5), it appears that the density of the fibrillar aggregates increases with field strength. At high concentration (HPT20), increase of field strength from 1 kV/mm to 3 kV/mm appears primarily to produce thickening of fibrils.

5.5 Conclusions

We have explored the electrorheological properties in steady shear flow of perchloric acid doped poly(3-thiophene acetic acid) (PTAA), particles suspended in silicone oil, examining the effects of field strength, particle concentration, doping degree (conductivity values), operating temperature, and nonionic surfactant on the yield stress. The PTAA/silicone oil suspensions show the typical ER response of Bingham flow behavior upon application of an electric field due to the formation of fibrillar agglomerates, induced by the electric polarization within particles, as confirmed by optical microscopy. In addition, the yield stress increases with electric field strength and particle volume fraction according to the power-law expression, $\tau_y \propto E^\alpha \phi^\gamma$. The scaling exponent α is close to the value of 2, predicted by the polarization model when the particle volume fraction is dilute and when the particle conductivity is low. The scaling exponent γ approaches the predicted value of unity when the electric field strength decreases. The yield stress initially increases with the operating temperature, probably due to conductivity enhancement with temperature, but becomes temperature independent above 25 °C. When the electric field strength is relatively weak, the yield stress does not depend on the presence of the surfactant. However, at electric fields above 1.5 kV/mm, the yield stress increases significantly, by up to 50%, on addition of small amounts of surfactant and then levels off at higher surfactant concentration.

5.6 Acknowledgements

The authors are grateful for the financial support provided by The Thailand Research Fund (TRF): TRF-RGJ grant no. PHD/0128/2542; and TRF-BGJ grant no. BGJ/03/2544. AMJ wishes to thank the National Science Foundation for support of this work through award DMR 0080114. We also wish to acknowledge Mr. Yiqiang Zhao, Mr. Shaosheng Dong, and Mr. Brian G. Olson of the Department of Macromolecular Science, Case Western Reserve University for fruitful discussion.

5.7 References

- Bonnecaze, R.T. and Brady, J.F. (1992). Yield stress in electrorheological fluids. J. Rheol., 36(1), 73-115.
- Barnes, H.A., Hutton, J.F., and Walters, K. (1989). **An Introduction to Rheology**. Amsterdam: Elsevier.
- Chen, L., Kim, B., Nishino, M., Gong, J., and Osada, Y. (2000). Environmental responses of polythiophene hydrogels. Macromolecules, 33(4), 1232-1236.
- Chin, B.D., Lee, Y.S., and Park, O.O. (1999). Dielectric and Rheological Behaviors of Semiconductive Polymer Suspension as an Electrorheological Fluid. Inter. J. Modern Phys B., 13, 1852-1859.
- Cho, M.S., and Choi, H.J. (2000). Scaling analysis of electrorheological poly(naphthalene quinone) radical suspensions. Korea-Australia Rheol. J., 12(3/4), 151-155.
- Cho, M.S., Kim, J.W., Choi, H.J., Webber, R.M., and Jhon, M.S. (2000). Electrorheological characteristics of polyaniline and its copolymer suspensions with ionic and nonionic substituents. Colloid Polym. Sci., 278(1), 61-64.
- Choi, H.J., Cho, M.S., and Kim, J.W. (2001). Electrorheology and universal yield stress function of semiconducting polymer suspensions. Korea-Australia Rheol. J., 13(4), 197-203.
- Choi, H.J., Cho, M.S., and To, K. (1998). Electrorheological and dielectric

- characteristics of semiconductive polyaniline-silicone oil suspensions. Physica A, 254, 272-279.
- Choi, H.J., Kim, J.W., Suh, M.S., Shin, M.J., and To, K. (2001). Synthesis and viscoelastic behavior of poly(aniline-co-ethoxyaniline) particles suspended electrorheological fluid. Inter. J. Modern Phys. B., 15, 649-656.
- Choi, H.J., Lee, J.H., Cho, M.S., Jhon, M.S. (1999). Electrorheological characterization of semiconducting polyaniline suspension. Polym. Eng. Sci., 39, 493.
- Choi, U.S. (1999). Electrorheological properties of chitosan suspension. Colloids Surf. A, 157, 193-202.
- Conrad, H., and Chen, Y. (1995). **Progress in Electrorheology: Science and Technology of Electrorheological Materials**. New York: Plenum.
- Cox, W.P., and Mertz, E.H. (1958). Correlation of dynamic and steady flow viscosities. J. Polym. Sci., 28, 619-622.
- Gonon, P., and Foulc, J.-N. (2000). Temperature dependence of particle-particle interactions in electrorheological fluids. J. Appl. Phys., 87, 3563-3566.
- Goodwin, J.W., Markham, G.M., and Vincent, B. (1997). Studied on model electrorheological fluids. J. Phys Chem. B, 101, 1961-1967.
- Gozdalik, A., Wycislik, H., and Plochanski, J. (2000). Electrorheological effect in suspensions of polyaniline. Synt. Met., 109, 147-150.
- Jang, W.H., Kim, J.W., Choi, H.J., and Jhon, M.S. (2001). Synthesis and electrorheology of camphorsulfonic acid doped polyaniline suspensions. Colloid Polym. Sci., 279(8), 823-827.
- Jun, J.B., Lee, C.H., Kim, J.W., and Suh, K.D. (2002). Synthesis and characterizations of monodispersed micron-sized polyaniline composite particles for electrorheological fluid materials. Colloid Polym. Sci., 280(8), 744-750.
- Kamath, G.M., and Wereley, N. (1997). A nonlinear viscoelastic-plastic model for electrorheological fluids. Smart Mater. Struct., 6, 351-359.
- Krause, S., and Katherine, B. (2001). Electromechanical response of electrorheological fluids and poly(dimethylsiloxane) networks. Macromolecules, 34(20), 7179-7189.

- Kim, B., Chen, L., Gong, J., and Osada, Y. (1999). Titration behavior and spectral transitions of water-soluble polythiophene carboxylic acids. Macromolecules, 32(12), 3964-3969.
- Kim, S.G., Kim, J.W., Choi, H.J., Suh, M.S., Shin, M.J., and Jhon, M.S. (2000). Synthesis and electrorheological characterization of emulsion-polymerized dodecylbenzenesulfonic acid doped polyaniline-based suspensions. Colloid Polym. Sci., 278(9), 894-898.
- Kim, Y.D., and Klingenberg, D.J. (1996). Two roles of nonionic surfactants on the electrorheological response. J. Colloid Interface Sci., 183(2), 568-578.
- Kim, Y.D., and Park, D.H. (2002). The electrorheological responses of suspensions of polypyrrole-coated polyethylene particles. Colloid Polym. Sci., 280(9), 828-834.
- Klingenberg, D.J., Swol, F.V., and Zukoshi, C.F. (1996) The small shear rate response of electrorheological suspensions: I. Simulation in the point-dipole limit. J. Chem. Phys., 94(9), 6160-6168.
- Klingenberg, D.J., Swol, F.V., and Zukoshi, C.F. (1996) The small shear rate response of electrorheological suspensions: II. Extension beyond the point-dipole limit. J. Chem. Phys., 94(9), 6170-6178.
- Klingenberg, D.J. and Zukoski C.F. (1990). Studies on the steady-shear behavior of electrorheological suspensions. Langmuir, 6(1), 15-24.
- Lan, Y., Xu, X., Men, S., and Lu, X. (1998). The conductivity dependence of the shear stress in electrorheological fluids. Appl. Phys. Lett., 73, 2908-2910.
- Langavola, A., Pavlinek, V., Saha, P., Stejskal, J., Kitano, T., and Quadrat, O. (2003). The effect of dielectric properties on the electrorheology of suspensions of silica particles coated with polyaniline. Physica A, 321(3&4), 411-424.
- Lee, H.J., Chin, B.D., Yang, S.M., and Park, O.O. (1998). Surfactant effect on the stability and electrorheological properties of polyaniline particle suspension. J. Colloid Interface Sci., 206, 424-438.
- Lee, J.H., Cho, M.S., Choi, H.J., and John, M.S. (1999). Effect of polymerization temperature on polyaniline based electrorheological suspensions. Colloid Polym. Sci., 277(1), 73-76.

- Lee Y.H., Kim C.A., Jang W.H., Choi H.J., Jhon M.S. (2001). Synthesis and electrorheological characteristics of microencapsulated polyaniline particles with melamine–formaldehyde resins. Polymer, 42(19), 8277-8283.
- Mavroidis, C., Pfeiffer, C., Celestino, C., and Cohen, Y.B. (2000). Controlled compliance haptic interface using electro-rheological fluids. Proceedings of the SPIE Smart Structures Conference, 3987, 1-11.
- Ma, Y., Zhang, Y., and Lu, K. (1998). Frequency and temperature dependence of complex strontium titanate electrorheological fluids under an alternating electric field. J. Appl. Phys., 83, 5522-5524.
- Parthasarathy, M., and Klingenberg, D.J. (1996). Electrorheology: Mechanisms and models. Mater. Sci. Eng.: R, 17(2), 57-103.
- Radcliffe, C.J., Lloyd, J.R., Andersland, R.M., and Hargrove, J.B. (1996). State Feedback Control of Electrorheological Fluids. Proceeding of ASME International Congress and Exhibition.
- Rankin, P.J., and Klingenberg, D.J. (1998). The electrorheology of barium titanate suspensions. J. Rheol., 42(3), 639-656.
- Sakurai, R., See, H., Saito, T., Asai, S., and Sumita, M. (1999). Suspension of layered particles: an optimum electrorheological fluid for d.c. applications. Rheol. Acta, 38(5), 478-483.
- Sim I.S., Kim J.W., and Choi H.J. (2001). Preparation and Electrorheological Characteristics of Poly(*p*-phenylene)-Based Suspensions. Chem. Mater., 13(4), 1243-1247.
- Sohn, J.I., Cho, M.S., Choi, H.J., and Jhon, M.S. (2002). Synthesis and electrorheology of semiconducting poly(naphthalene quinone) radical particles. Macromol. Chem. Phys., 203, 1135-1141.
- Sung, J.H., Choi, H.J., Sohn, J.I., and Jhon, M.S. (2003). Electrorheology of chitosan polysaccharide suspensions in soybean oil. Colloid Polym. Sci., 281(12), 1196-1200.
- Voyles, R.M., Fedder, G., and Khosla, P.K. (1996). Design of a modular tactile sensor and actuator based on an electrorheological gel. Proceeding of the 1996 IEEE International Conference on Robotics and Automation, 13-17.
- Weiss, K. D., and Duclos, T. G. (1994). Controllable Fluids: The Temperature

Dependence of Post-Yield Properties. Int. J. Mod. Phys. B, 8, 3015-3030.

Wu, C. W., and Conrad, H. (1998). The temperature dependence of the conductivity of silicone oil and related electrorheology of suspensions containing zeolite particles. J. Phys. D: Appl. Phys., 31, 3403-3409.

Zhao, X.P., and Yin, J.B. (2002). Preparation and Electrorheological Characteristics of Rare-Earth-Doped TiO₂ Suspensions. Chem. Mater., 14(5), 2258-2263.

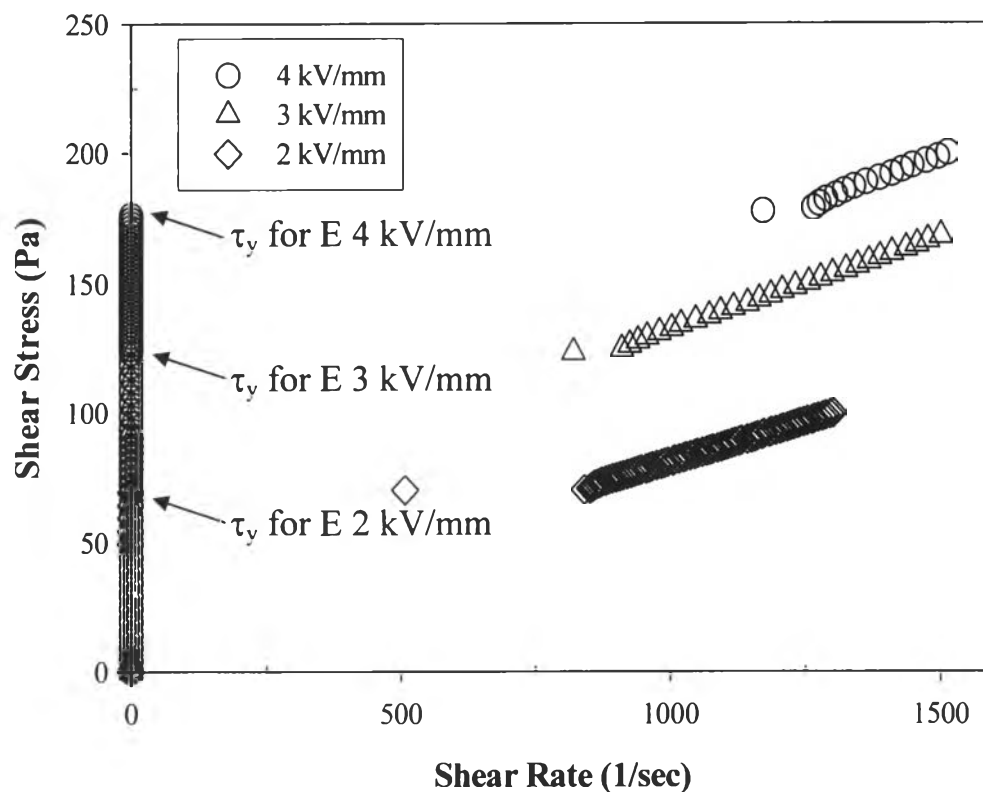


Figure 5.1 Measurement of the static yield shear stress with different electric field strengths using controlled shear stress sweep for 5 wt % highly doped polythiophene suspension (HPT5) at 25 °C.

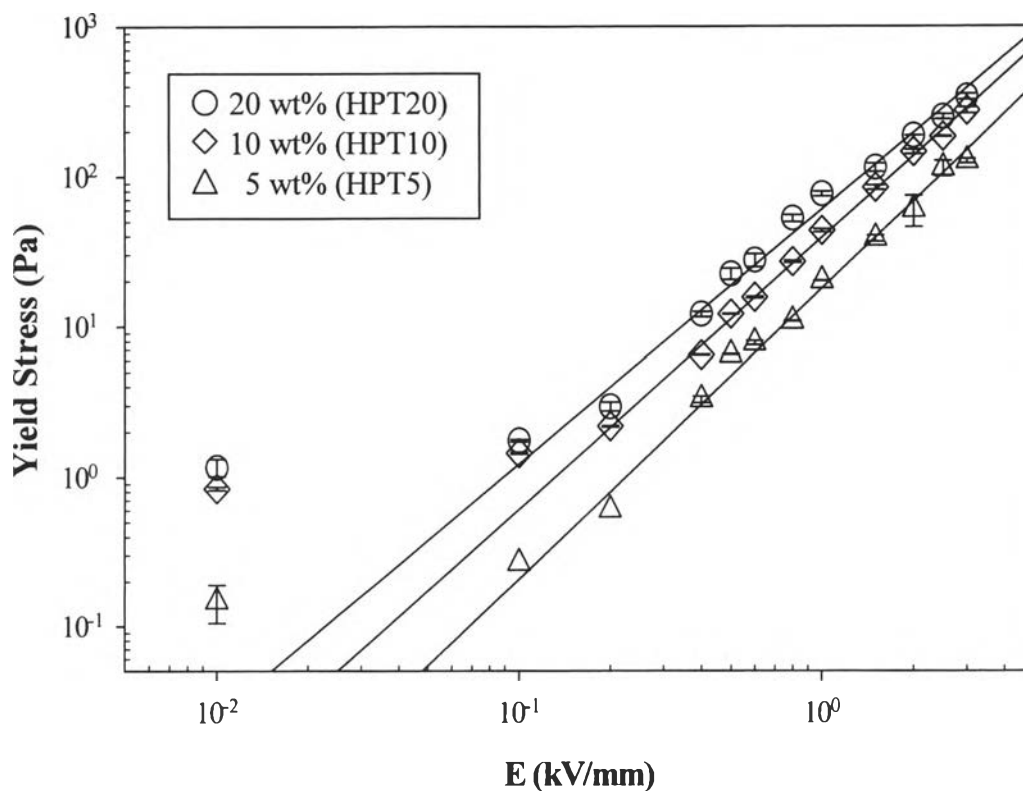


Figure 5.2 Effect of particle concentration on the static yield stress of highly doped polythiophene suspensions at various electric field strengths. The lines indicate least squares fits to a power-law which yields scaling exponent values, α , of 1.94, 1.81, and 1.69, for the HPT5, HPT10, and HPT20 suspensions, respectively.

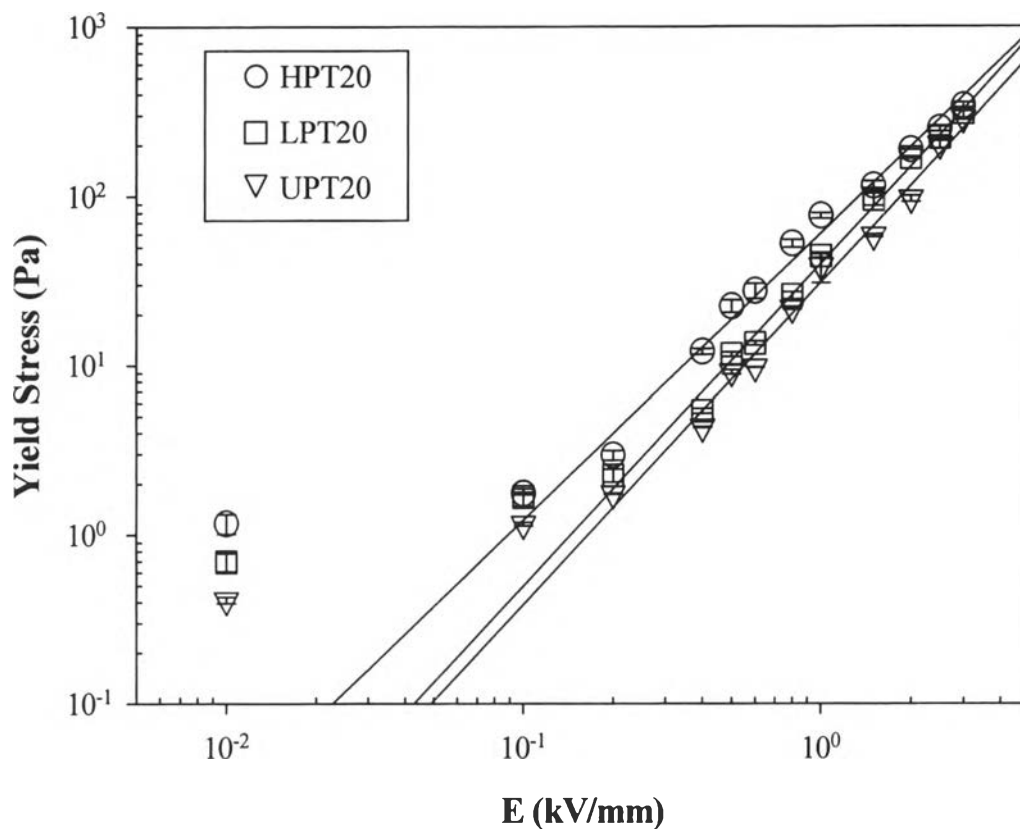


Figure 5.3 Effect of particle conductivity on the static yield stress of 20 wt % HClO₄ doped polythiophene suspension at various electric field strengths; (O) HPT20, (□) LPT20, and (▽) undoped polythiophene. The lines indicate least squares fits to a power-law which yields scaling exponent values, α , of 1.90, 1.90, and 1.69 for the UPT20, LPT20, and HPT20 suspensions, respectively.

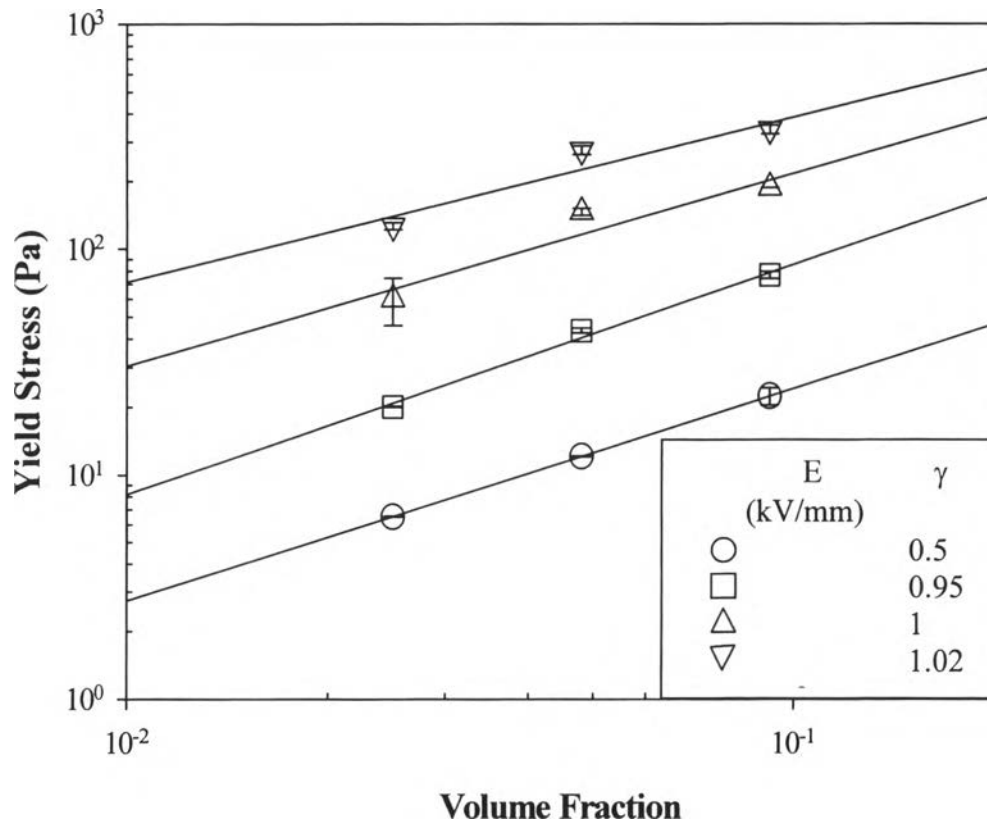


Figure 5.4 The dependence of the static yield stress on electric field strength for different volume fractions of highly doped polythiophene suspension (HPT) at 25 °C.

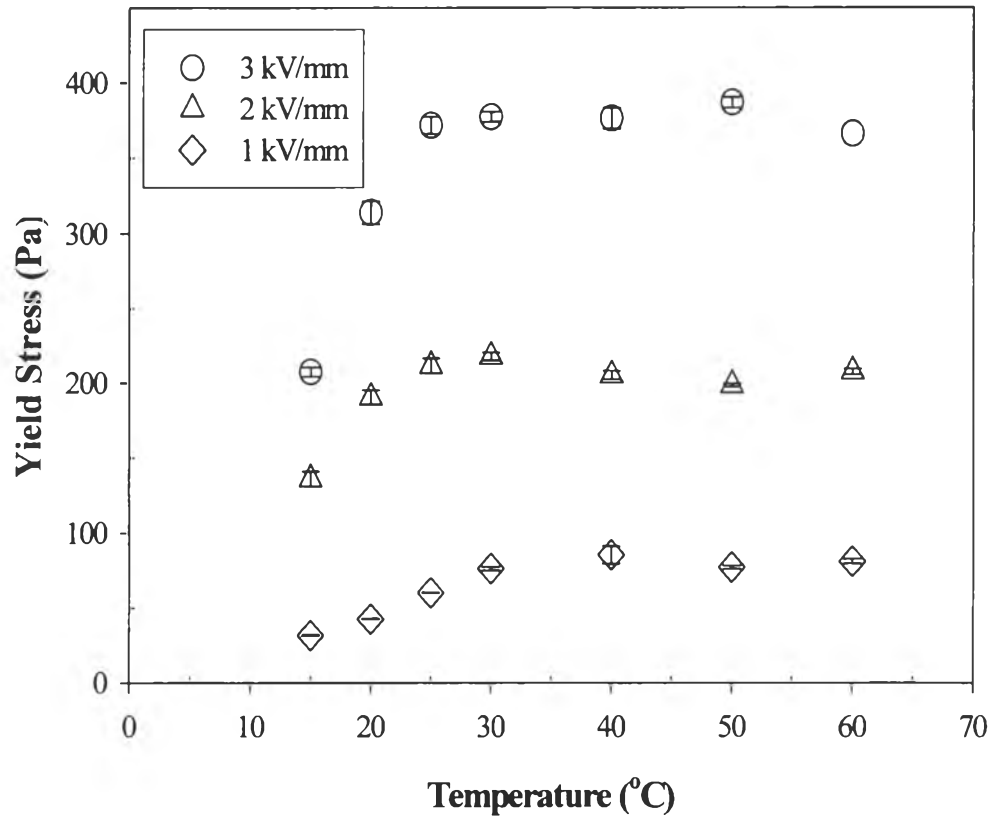


Figure 5.5 The effect of operating temperature on static yield stress of 20 wt % HClO₄ doped polythiophene suspension (HPT20) at various electric field strengths.

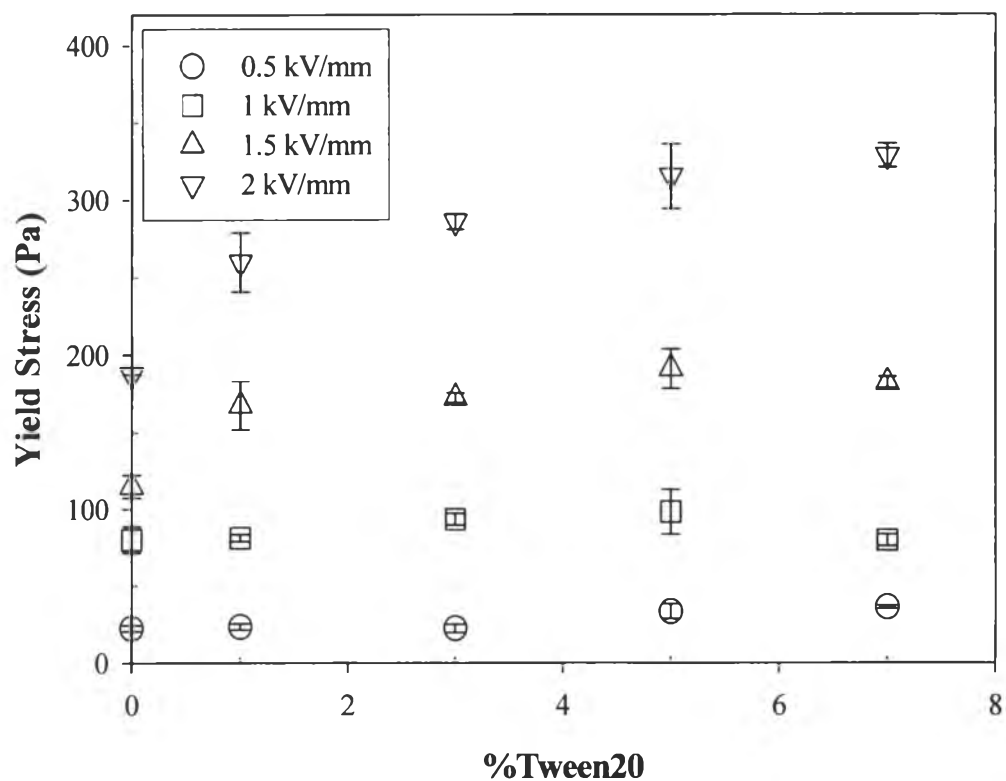


Figure 5.6 Effect of addition of Tween20 on the static yield stress of 20 wt % HClO4 doped polythiophene suspension (HPT20) at various electric field strengths.

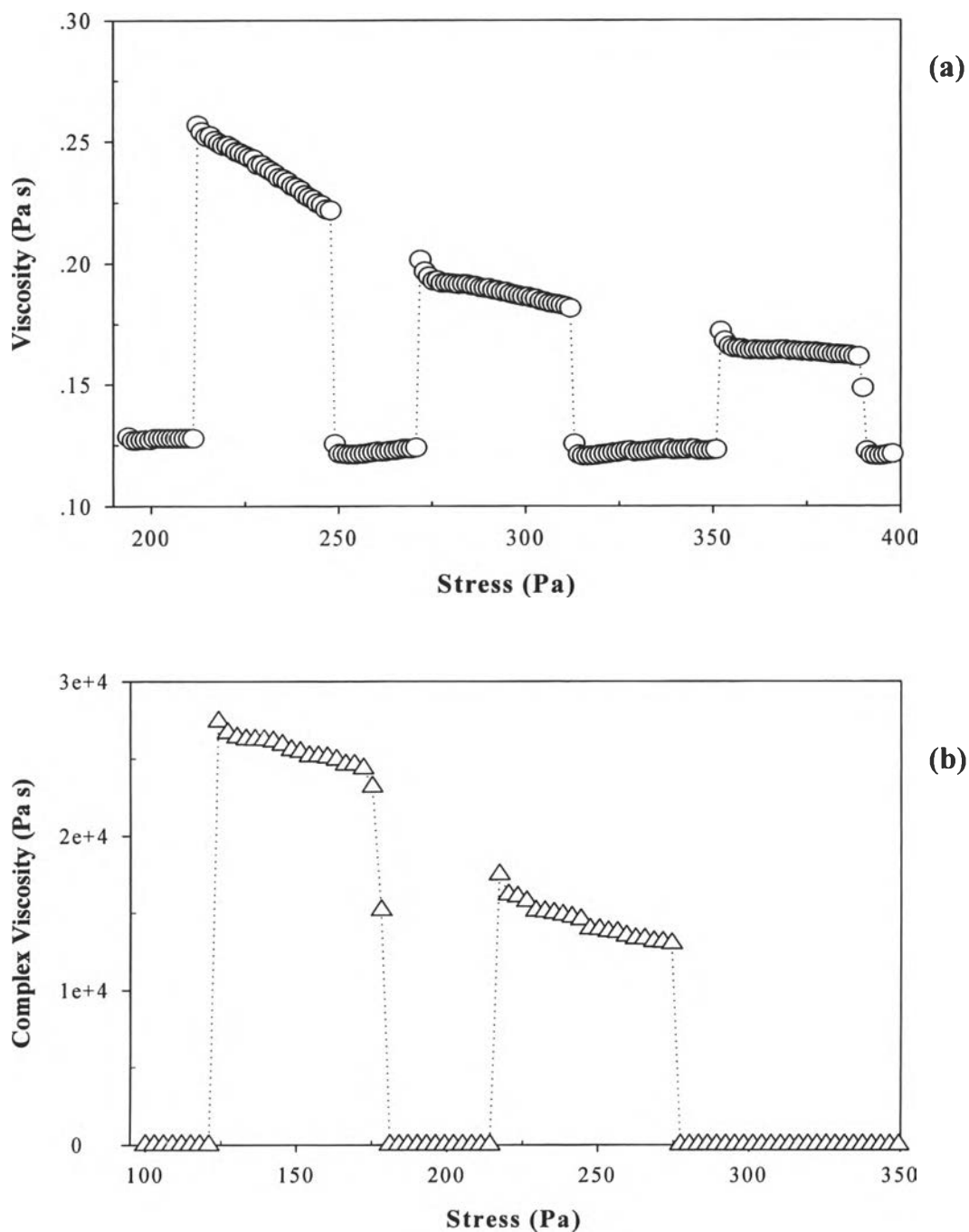


Figure 5.7 Effect of switching the applied electric field on the viscosity of a 20 wt % highly HClO₄ doped polythiophene suspensions during stress sweep test at 25 oC: an applied field of 2 kV/mm is switched on and off alternately; (a) steady shear viscosity and (b) complex viscosity.

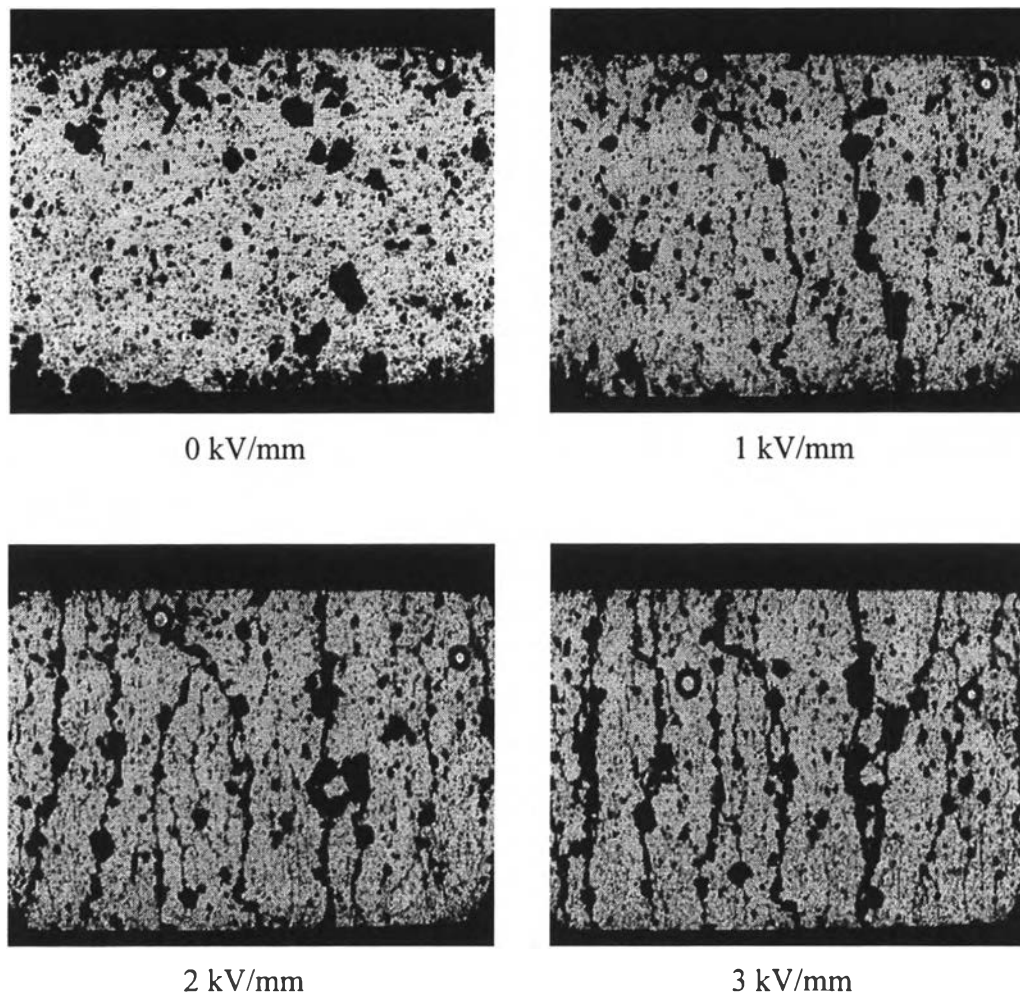


Figure 5.8 Optical micrographs of 5 wt % highly doped PTAA/silicone oil suspension (HPT5) at various electric field strengths under quiescent conditions.

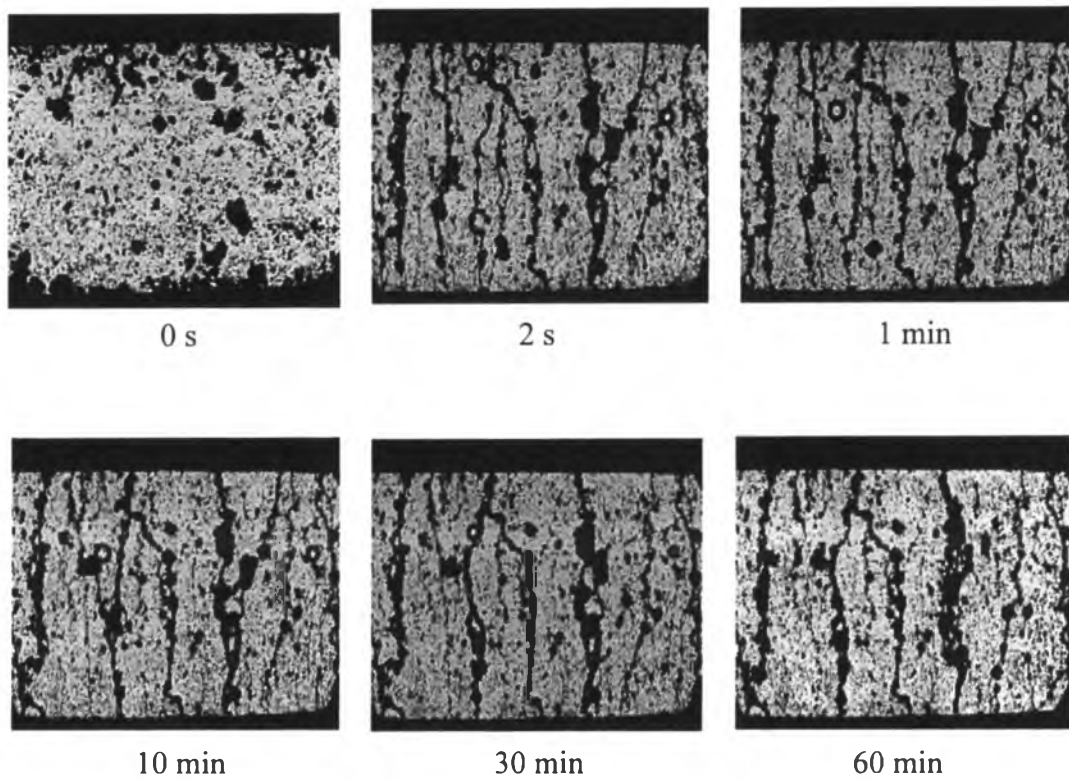


Figure 5.9 Optical micrographs of HPT5 under quiescent conditions, following application of a constant electric field of 3 kV/mm.

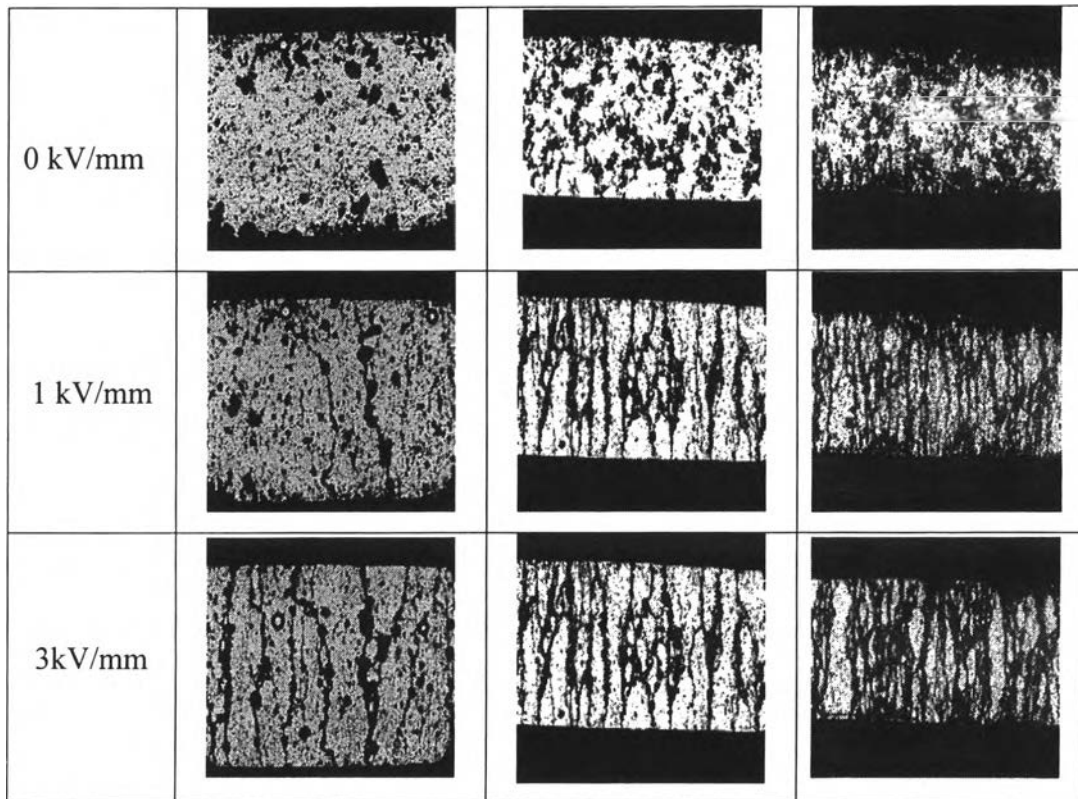


Figure 5.10 Optical micrographs of highly doped PTAA/silicone oil suspensions (HPT) under quiescent conditions at different particle concentrations and electric field strength.